Effects of modal incompleteness on quantification of mode shapes complexity in vibrating structures

IOP Conf. Series: Journal of Physics: Conf. Series **1264** (2019) 012054 doi:10.1088/1742-6596/1264/1/012054

Effects of modal incompleteness on quantification of mode shapes complexity in vibrating structures

F Iezzi[1] and C Valente[1]

[1]Department of Engineering and Geology, University "G. d'Annunzio" of Chieti-Pescara, Viale Pindaro 42, 65127 Pescara, Italy

E-mail: fabrizio.iezzi@unich.it

Abstract. In experimental modal analysis, the mode shapes turn out to be complex due to the non-proportionality of damping in actual structures. For identification purposes, several indices have been proposed to quantify this complexity. Unfortunately, the effectiveness of the above indices is affected by the problem of data incompleteness that arises when a limited set of modal data is available, as in the case of reduced eigenvector components or in the case of band limited eigenvalues range. In contexts such as model updating, this problem makes it difficult to pair experimental versus numerical data and methods to compare the two sets of data are based on the reduction of numerical models or, conversely, on the expansion of the experimental one. However none of them reveals completely satisfactory. The present work aims to analyze the effectiveness of the above modal complexity indices. To this end, the most sensitive index found from previous studies is used in order to detect the mode shapes complexity compared to the damping non-proportionality in vibrating structures for different levels of modal incompleteness.

1. Introduction

The viscous damping in vibrating structures can be proportional or non-proportional, depending whether the damping matrix is a combination of the mass and stiffness matrices or not [1]. In the first case, the mode shapes are real and the degrees of freedom (dofs) of the system oscillate in phase whereas, in the second case, the mode shapes are complex and the dofs oscillate out of phase [2].

Therefore, the imaginary content of the mode shapes can be used for the quantification of the non-proportional damping. Several indices exist on purpose to provide estimates of the modal complexity and then of the damping non-proportionality [3]–[4]. These indices are zero for real mode shapes and increase along with the imaginary content of the mode shapes. As shown in [3]–[4], the indices can be divided in two groups depending on their identifiability: unmeasurable indices and measurable indices. The unmeasurable indices require the knowledge of the damping matrix of the system, which is not identifiable directly from experimental tests; therefore, they have essentially theoretical value since they cannot be experimentally derived. On the contrary, the measurable indices require the knowledge of the modes shapes of the system, which can be identified directly from experimental tests. Consequently, from a practical point of view, only the measurable indices are experimentally useful, even if their identification and effectiveness suffer for two problems: modal density and data incompleteness. The first problems is typical of the case in which the structures vibrate with close spaced frequencies and this circumstance affects the experimental identification of the mode shapes regardless the accuracy of the method used for the identification; as consequence, depending on the modal density, a fictitious

over-content of the imaginary part of the mode shapes is detected, as demonstrated in [4]–[6]. The second problem arises in the case of availability of a limited set of modal data or when the band of the eigenvalues range is limited because of, respectively, the structural response is estimated only in limited numbers of measured points (or dofs) and on a limited range of frequencies of the vibrating structure.

In contexts such as model updating, this problem makes it difficult to pair experimental versus numerical data and methods to compare the two sets of data are based on the reduction of numerical models or, conversely, on the expansion of the experimental results.

The present work aims to analyze the effectiveness of the above modal complexity indices. To this end, the most sensitive index found from previous studies [7]–[10] is used in order to detect the mode shapes complexity in vibrating structures for different levels of modal incompleteness. The method based on the reduction of the mass, stiffness and damping matrices of the numerical model dofs of the structure [11] is followed.

2. Matrices reduction procedure

In the literature there are several different procedures for the reduction of the mass, stiffness and damping matrices via the reduction of the dofs of a numerical model [12] necessary for the comparison between the experimental and numerical modal parameters of a structure in vibration. Among these, the most common is the Guyan reduction procedure [13] that applies in problems of modal analysis of undamped structures, and so endowed with real mode shapes. The relevant dynamics is described by the equation of motion:

$$\mathbf{M}\ddot{\mathbf{x}} + \mathbf{K}\mathbf{x} = \mathbf{P}(t) \tag{1}$$

in which t is the time variable; $\mathbf{x}$ and $\ddot{\mathbf{x}}$ are, respectively, the displacement and acceleration vectors; $\mathbf{M}$ and $\mathbf{K}$ are the mass and stiffness matrices, respectively; $\mathbf{P}$ is the external forces vector.

For the purpose of the present work, the Guyan reduction is extended to damped structures governed by the following equation of motion:

$$\mathbf{M}\ddot{\mathbf{x}} + \mathbf{C}\dot{\mathbf{x}} + \mathbf{K}\mathbf{x} = \mathbf{P}(t) \tag{2}$$

where $\dot{\mathbf{x}}$ is the velocity vector and $\mathbf{C}$ is the damping matrix. This matrix $\mathbf{C}$ can be proportional or not to $\mathbf{M}$ and $\mathbf{K}$ and so the mode shapes result real or complex, respectively.

For the case of the equation (2), the $\mathbf{x}$, $\dot{\mathbf{x}}$, $\ddot{\mathbf{x}}$ vectors are partitioned in two sub-vectors depending on the measured and unmeasured dofs. The matrices $\mathbf{M}$, $\mathbf{C}$ and $\mathbf{K}$ and the vector $\mathbf{P}$ are partitioned accordingly. If the external forces are not in correspondence of the unmeasured dofs, the equation (2) becomes:

$$\begin{bmatrix} \mathbf{M}_{mm} & \mathbf{M}_{mn} \\ \mathbf{M}_{nm} & \mathbf{M}_{nn} \end{bmatrix} \begin{bmatrix} \ddot{\mathbf{x}}_m \\ \ddot{\mathbf{x}}_n \end{bmatrix} + \begin{bmatrix} \mathbf{C}_{mm} & \mathbf{C}_{mn} \\ \mathbf{C}_{nm} & \mathbf{C}_{nn} \end{bmatrix} \begin{bmatrix} \dot{\mathbf{x}}_m \\ \dot{\mathbf{x}}_n \end{bmatrix} + \begin{bmatrix} \mathbf{K}_{mm} & \mathbf{K}_{mn} \\ \mathbf{K}_{nm} & \mathbf{K}_{nn} \end{bmatrix} \begin{bmatrix} \mathbf{x}_m \\ \mathbf{x}_n \end{bmatrix} = \begin{bmatrix} \mathbf{P}_m \\ \mathbf{0} \end{bmatrix} \tag{3}$$

in which the subscript m and n are referred, respectively, to the measured and unmeasured dofs. In the case of static reduction, the inertial and dissipative components are neglected and the equation (3) takes the form:

$$\mathbf{K}_{nm}\mathbf{x}_m + \mathbf{K}_{nn}\mathbf{x}_n = \mathbf{0} \tag{4}$$

that can be used to get the results of the unmeasured dofs as a function of the measured ones, in the following way:

$$\begin{bmatrix} \mathbf{x}_m \\ \mathbf{x}_n \end{bmatrix} = \begin{bmatrix} \mathbf{I} \\ -\mathbf{K}_{nn}^{-1}\mathbf{K}_{nm} \end{bmatrix} \mathbf{x}_m = \mathbf{T}\mathbf{x}_m \tag{5}$$

where $\mathbf{I}$ is the identity matrix and $\mathbf{T}$ corresponds to the static transformation between the complete displacements vector $[\mathbf{x}_m; \mathbf{x}_n]^T$ (i.e. formed by the measured and unmeasured dofs) and the incomplete one $[\mathbf{x}_m]^T$ (i.e. formed by only the measured dofs).

The reduced mass, damping and stiffness matrices are given by:

$$\mathbf{M}_R = \mathbf{T}^T\mathbf{M}\mathbf{T};\quad \mathbf{C}_R = \mathbf{T}^T\mathbf{C}\mathbf{T};\quad \mathbf{K}_R = \mathbf{T}^T\mathbf{K}\mathbf{T} \tag{6}$$

in which $\mathbf{M}_R$, $\mathbf{C}_R$ and $\mathbf{K}_R$ are, respectively, the reduced **M**, **C** and **K**.

It is important to note that the Guyan reduction provides exact solutions only in the case of null frequencies (static field). In fact, with the increase of the frequencies of the structure (dynamic field), the neglected contributions of the inertial and dissipative components in equation (2) increases and so the accuracy of the modal identification decreases.

3. Case study and methodology

The effects of the modal data incompleteness on the modal complexity quantification in vibrating structures are analyzed using as data generator a basic model of a framed structure with the scheme of "weak column - strong beam".

The reference structure is a plane frame with a single span and ten levels (figure 1). The inter-storey height is 3 m and a mass m of 10 t is condensed at each level. The columns have a constant cross-section 0,30 by 0,30 m and a Young modulus equal to $3 \cdot 10^7$ kN/m^2, so the inter-storey stiffness k is $1{,}8 \cdot 10^4$ kN/m. The dynamics of this structures is described by the equation (2).

For simplicity, the matrix **C** is taken equal to $\mathbf{C} = \beta\mathbf{K}$ for proportional damping and to $\mathbf{C} \neq \beta\mathbf{K}$ for non-proportional damping.

In case of damping proportionality, the three conditions $\mathbf{K}\mathbf{M}^{-1}\mathbf{C} = \mathbf{C}\mathbf{M}^{-1}\mathbf{K}$, $\mathbf{M}\mathbf{K}^{-1}\mathbf{C} = \mathbf{C}\mathbf{K}^{-1}\mathbf{M}$, $\mathbf{M}\mathbf{C}^{-1}\mathbf{K} = \mathbf{K}\mathbf{C}^{-1}\mathbf{M}$ posed in [14] to ensure the proportional damping existence are in fact satisfied and, consequently, the mode shapes are real and the modal complexity indices must be zero. On the contrary, in case of non-proportional damping the above three conditions for the proportional damping existence are not satisfied, therefore the mode shapes are complex and the modal complexity indices must be different than zero.

More in detail, in the present reference structure, the non-proportional damping is generated using a non-proportionality factor $f_c \geq 1$ that multiplies the damping coefficient c of the first inter-storey. For $f_c = 1$, **C** is proportional (real mode shapes) whereas for $f_c > 1$, **C** is non-proportional (complex mode shapes). The non-proportionality (and therefore the mode complexity) increases along with the f_c increase. It is assumed $\beta = 0{,}0223$ so that for proportional **C**, the damping ratio is equal to 5% for the first mode shape and the damping coefficient takes the value $c = 401{,}4$ kNs/m.

In order to detect the mode shapes complexity for different levels of modal incompleteness, among all the measurable indices, the most sensitive index is used [3]. This index I is the modal imaginary ratio; it weighs the imaginary part with respect to the overall length of the mode shape and its explicit expression is reported below:

$$I = \frac{\|\mathrm{Im}(\boldsymbol{\Psi}_r)\|}{\||\boldsymbol{\Psi}_r|\|} \tag{7}$$

where $\boldsymbol{\Psi}_r$ is the r-th mode shape; $\mathrm{Im}(\boldsymbol{\Psi}_r)$ stands for the imaginary part of $\boldsymbol{\Psi}_r$, whereas $\|\cdot\|$ is the Euclidean 2-norm operator and $|\cdot|$ is intended as the componentwise absolute value.

In order to work in a controlled environment, the index I is tested on theoretical data. The theoretical mode shapes are derived using the standard modal analysis according to the state space method to deal with the non-proportional damping [15]:

$$(\mathbf{B} - \lambda\mathbf{A})\mathbf{Z} = \mathbf{0};\quad [\mathbf{A}] = \begin{bmatrix}\mathbf{C} & \mathbf{M}\\ \mathbf{M} & \mathbf{0}\end{bmatrix};\quad [\mathbf{B}] = \begin{bmatrix}\mathbf{K} & \mathbf{0}\\ \mathbf{0} & -\mathbf{M}\end{bmatrix};\quad [\mathbf{Z}] = \begin{bmatrix}\mathbf{x}\\ \dot{\mathbf{x}}\end{bmatrix} \tag{8}$$

in which λ is the generic eigenvalue and **Z** the state space vector.

The mode shapes used to compute the index I are then treated according to the procedure in [16] to ensure the minimization of the errors in the identification of the imaginary part of the mode shapes; geometrically, this procedure corresponds to a rigid rotation of the complex mode shape in the complex plane such that it optimally aligns with the real axis.

Finally, the index I, scaled in the interval [0; 1] and expressed in percentage, is analyzed to infer the effects of the modal incompleteness on the complexity of the mode shapes.

To discuss the influence of the modal data incompleteness on the index *I*, the mode shapes endowed with the greater energy contribution on the overall motion of the structure are analyzed, these are the first, second and third mode shape. In particular, for each mode shape, the index *I* is estimated for the simultaneous increase of incompleteness and damping non-proportionality. To do that the coefficient *c* of the first inter-storey is gradually scaled by the multiplicative factor $f_c \geq 1$, in the range $f_c = [1; 2]$ in order to have a maximum damping ratio equal to 30% in the third mode shape. Then the modal incompleteness is increased by progressively reducing the measured dofs number, to pass from an initial condition of 10 dofs to a final condition of 5 dofs measured (figure 1). The considered cases are: 10 dofs measured (case 0; all the dofs are measured); 9 dofs measured (case 1: the dof 3 is unmeasured); 8 dofs measured (case 2: the dofs 3 and 8 are unmeasured); 7 dofs measured (case 3: the dofs 2, 5 and 8 are unmeasured); 6 dofs measured (case 4: the dofs 2, 4, 6 and 8 are unmeasured); 5 dofs measured (case 5: the dofs 2, 4, 6, 8 and 9 are unmeasured).

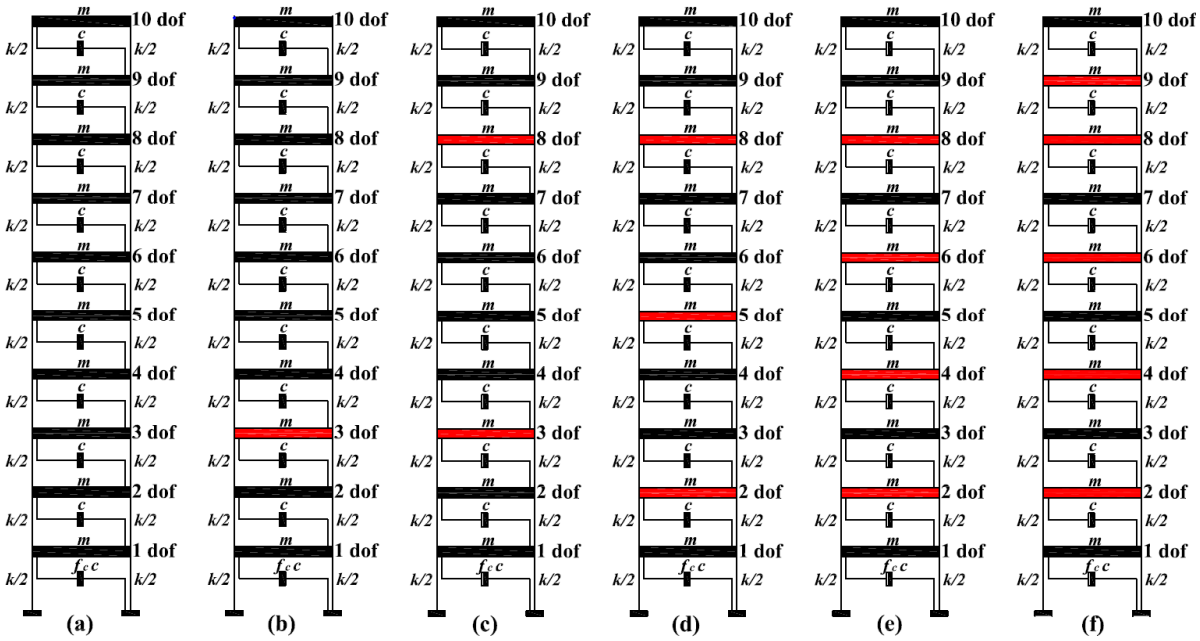

Figure 1. (a) Reference structure case 0; (b) case 1; (c) case 2; (d) case 3; (e) case 4; (f) case 5: measured (black) and unmeasured (red) dofs. Structure parameters: m = 10 t; k = 1,8·10^4 kN/m; c = 401,4 kNs/m; $f_c = [1; 2]$.

4. Results

In the figures below, the values attained by the index *I* as function of the factor f_c are reported respectively for the first (figure 2), second (figure 3) and third (figure 4) mode shape of the reference structure with respect to the variation of the number of the measured dofs.

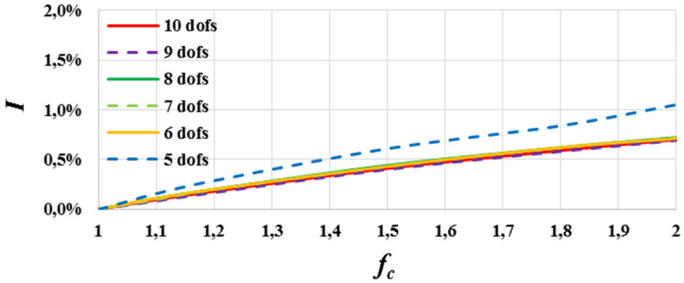

Figure 2. Mode shape 1: modal complexity index *I* (vertical axis) versus non-proportionality damping factor f_c (horizontal axis) with respect to the measured dofs number (from 10 to 5).

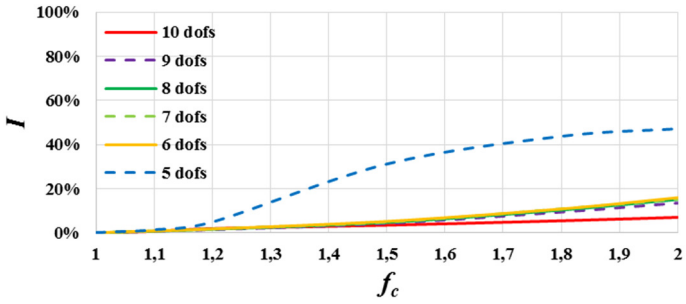

Figure 3. Mode shape 2: modal complexity index I (vertical axis) versus non-proportionality damping factor f_c (horizontal axis) with respect to the measured dofs number (from 10 to 5).

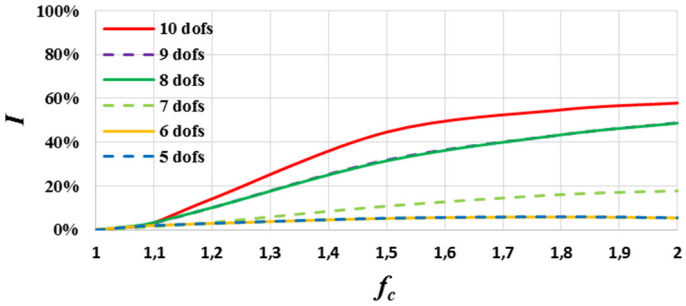

Figure 4. Mode shape 3: modal complexity index I (vertical axis) versus non-proportionality damping factor f_c (horizontal axis) with respect to the measured dofs number (from 10 to 5).

By means of the figures from 2 to 4 it is clear that for each mode shapes the trend of the index I deviates progressively along with the reduction of the measured dofs. For each mode shape, in general, the index I is a monotonic function increasing with f_c independently from the measured dofs number. This condition is coherent with the increase of the imaginary part of the mode shapes because of the increase of the damping non-proportionality in the vibrating structure.

In the case of the first mode shape (figure 2) the index I deviates in a relatively limited way with respect to the corresponding index I estimated using all the measured dofs. More in detail, with the decrease of the measured dofs number, the index I augments regardless of the f_c value. The index I trends are quasi-linear functions respect to f_c; therefore the index I is endowed of constant and not high sensitivity to the damping non-proportionality.

The results found for the first mode shape (figure 2) extend qualitatively also to the second mode shape (figure 3). In the case of the second mode shape, however, the curve relative to the index I with 5 measured dofs results as peculiar case. This curve, in fact, shows an important deviation and notably larger values respect to all the other curves; furthermore, it loses the quasi-linear growth showing a variable sensitivity: limited for f_c = {[1; 1,3) U (1,6; 2]} and high for f_c = [1,3; 1,6].

In the case of the third mode shape (figure 4), a reverse behavior of the index I is observed with respect to the results involving the first and second mode shape. In particular, the index I decreases along with the reduction of the unmeasured dofs number. Nonetheless, it is important to note that the modal complexity quantity (i.e. the index I) preserves the fundamental feature to increase along with the increase of the damping non-proportionality (i.e. of the factor f_c).

The results shown in the figures from 2 to 4 can also be explained via the correlation analysis between the complete and the incomplete mode shapes for a given damping level f_c. The use of the MAC index (Modal Assurance Criterion) is one of the most common technique to assess the correlation degree between mode shapes [17]. The comparison between the r-th complete mode shape $\{\mathbf{Z}_C\}_r$ (identified using a number of measured dofs equal to 10) and the s-th incomplete mode shape ($\{\mathbf{Z}_I\}_s$ (identified using a number of measured dofs less than 10) is given by:

$$\mathrm{MAC}_{CI} = \frac{(\{\mathbf{Z}_C\}_r \cdot \{\mathbf{Z}_I\}_s)^2}{(\{\mathbf{Z}_C\}_r^T \cdot \{\mathbf{Z}_C\}_r) \cdot (\{\mathbf{Z}_I\}_s^T \cdot \{\mathbf{Z}_I\}_s)} \tag{9}$$

where, in order to get a meaningful operation, $\{\mathbf{Z}_C\}_r$ is preliminary mapped into the $\{\mathbf{Z}_I\}_s$ subspace.

It is worth recalling that the MAC_{CI} index takes values in the interval [0; 1]: a value close to 0 indicates a low correlation, whereas a value equal to 1 represents a perfect correlation between two mode shapes. Generally, the correlation can be considered satisfactory for MAC_{CI} values higher than 0,8.

In order get a synthetic and simultaneous view of the comparison among various mode shapes, the MAC_{CI} values are collected into a specific matrix that, in the ideal case, should be a diagonal matrix composed by 1 in the main diagonal and 0 elsewhere. In the present context, due to the complexity of the mode shapes, the MAC_{CI} indices are characterized by complex numbers too.

Aiming at analyze the correlation between the complete $\{\mathbf{Z}_C\}_r$ and the incomplete $\{\mathbf{Z}_I\}_s$ mode shapes (r, s = 1st, 2nd, 3rd mode shape), the 3D bar graph representation of the MAC_{CI} matrix entries is adopted on purpose. This representation is shown separately for the real and imaginary parts of the MAC_{CI} matrix where the x, y, z, axis stand, respectively, for the three complete mode shapes, the three incomplete mode shapes and the real or imaginary part of the MAC_{CI} indices.

To highlight the results of the correlations, only the results relative to the limit cases of f_c (f_c = 1 and f_c = 2) and of measured dofs number are reported and discussed below. The detail of the considered cases is as follows: correlation between the mode shapes identified using 10 dofs (complete mode shapes) and 9 (incomplete mode shapes) measured, for f_c = 1 (figures 5, 6) and f_c = 2 (figures 7, 8), using 10 dofs (complete mode shapes) and 5 (incomplete mode shapes) measured, for f_c = 1 (figures 9, 10) and f_c = 2 (figures 11, 12).

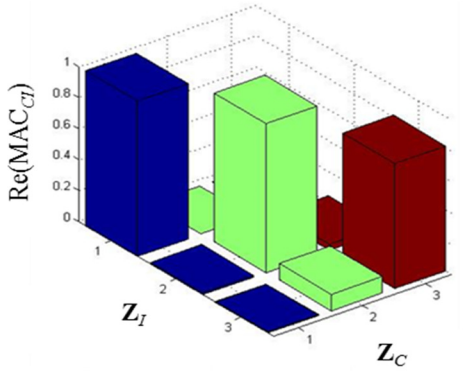

Figure 5. Real part of the MAC_{CI} index between the 1st, 2nd and 3rd complete $\mathbf{Z}_C$ (identified with 10 dofs) and incomplete $\mathbf{Z}_I$ (identified with 9 dofs) mode shapes for f_c = 1.

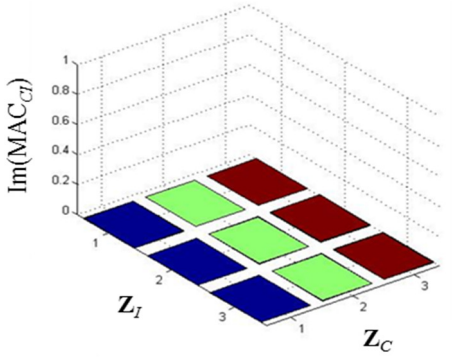

Figure 6. Imaginary part of the MAC_{CI} index between the 1st, 2nd and 3rd complete $\mathbf{Z}_C$ (identified with 10 dofs) and incomplete (identified with 9 dofs) mode shapes $\mathbf{Z}_I$ for f_c = 1.

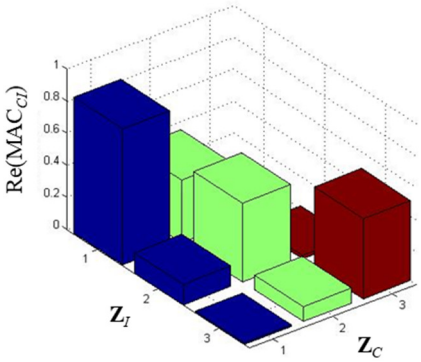

Figure 7. Real part of the MAC_{CI} index between the 1st, 2nd and 3rd complete $\mathbf{Z}_C$ (identified with 10 dofs) and incomplete $\mathbf{Z}_I$ (identified with 9 dofs) mode shapes for f_c = 2.

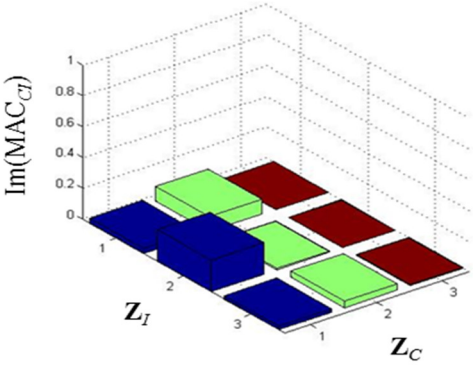

Figure 8. Imaginary part of the MAC_{CI} index between the 1st, 2nd and 3rd complete $\mathbf{Z}_C$ (identified with 10 dofs) and incomplete $\mathbf{Z}_I$ (identified with 9 dofs) mode shapes for f_c = 2.

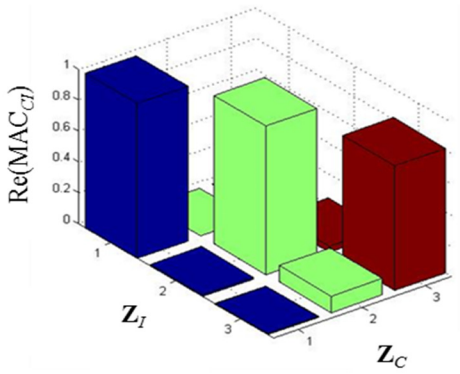

Figure 9. Real part of the MAC_{CI} index between the 1st, 2nd and 3rd complete $\mathbf{Z}_C$ (identified with 10 dofs) and incomplete $\mathbf{Z}_I$ (identified with 5 dofs) mode shapes for $f_c = 1$.

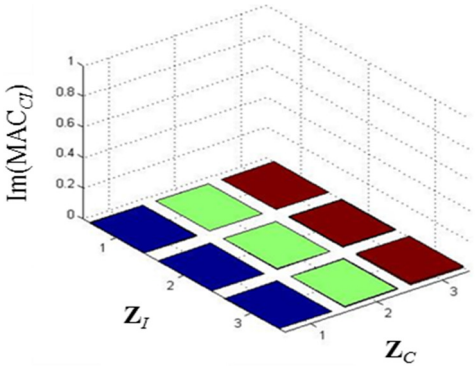

Figure 10. Imaginary part of the MAC_{CI} index between the 1st, 2nd and 3rd complete $\mathbf{Z}_C$ (identified with 10 dofs) and incomplete $\mathbf{Z}_I$ (identified with 5 dofs) mode shapes for $f_c = 1$.

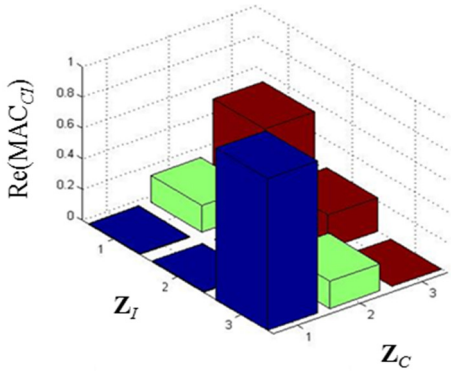

Figure 11. Real part of the MAC_{CI} index between the 1st, 2nd and 3rd complete $\mathbf{Z}_C$ (identified with 10 dofs) and incomplete $\mathbf{Z}_I$ (identified with 5 dofs) mode shapes for $f_c = 2$.

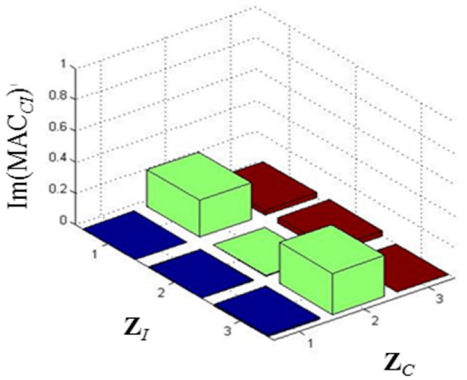

Figure 12. Imaginary part of the MAC_{CI} index between the 1st, 2nd and 3rd complete $\mathbf{Z}_C$ (identified with 10 dofs) and incomplete $\mathbf{Z}_I$ (identified with 5 dofs) mode shapes for $f_c = 2$.

The comparison among the figures 5 to 12 allows to trace the following considerations. As long as the damping is proportional ($f_c = 1$) the $Im(MAC_{CI})$ is equal to 0 (figures 6 and 10), regardless the modal completeness; whereas the $Re(MAC_{CI})$ is close to 1 along the main diagonal and practically 0 elsewhere (figures 5 and 9) witnessing the correlation between $\{\mathbf{Z}_C\}_r$ and $\{\mathbf{Z}_I\}_s$. When the damping becomes non-proportional ($f_c = 2$) the imaginary part of the MAC_{CI} matrix presents entries sensibly different than 0 (figures 8 and 12). Therefore, the only responsible for the appearance of complexity is the level of damping non-proportionality. Conversely, it is hence possible to distinguish the presence of non-proportionality by the level of mode shape complexity regardless the modal shape completeness.

5. Conclusions

In the experimental modal identification of actual vibrating structures, the mode shapes complexity is related to the entity of damping non-proportionality. This complexity increases along with the non-proportionality increase of the damping. In the literature several indices exist to estimate the modal complexity and hence the level of non-proportional damping. These indices are formulated using the mode shapes as basic data and present different sensitivity in detecting the modal complexity. For definiteness, in the present work, the most effective index found by previous studies (the modal

imaginary ratio) is employed. Such index weighs the importance of the imaginary part with respect to the overall length of the complex mode shape.

Identification problems can arise due to the modal data incompleteness since this latter can artificially affect the complexity level of the mode shapes. These kind of problems should be taken into account not only in the present context, but in all cases in which two quantities should be paired as, for instance, in the case of modal updating procedures. In the present work, the above concepts are discussed according to an appropriate case study consisting in a framed structure model.

The analysis of the index trend shows that, even if the modal data incompleteness affects the complexity of a mode shape, the fundamental behavior of the index preserves the monotonic features displayed in the case of modal completeness. In fact, the index presents a one to one correspondence with the damping non-proportionality regardless of the modal data incompleteness.

References

[1] Chopra A K 2012 *Dynamics of Structures* 4th ed (USA: Prentice Hall/Pearson).
[2] Craig R R and Kurdila A J 2006 *Foundamentals of Structural Dynamics* 2nd ed (USA: Wiley).
[3] Iezzi F 2016 Structural damage identification via the modal complexity (in Italian), *PhD Thesis*, University "G. d'Annunzio" of Chieti-Pescara, Italy.
[4] Iezzi F and Valente C 2017 Modal density influence on modal complexity quantification in dynamic systems *Procedia Engineering* 199(2017) pp 942–947.
[5] Gabriele S, Iezzi F, Spina D and Valente C 2014 The effects of modal density in system identification using the Hilbert transform *Proceedings of 2014 IEEE Workshop on Environmental, Energy and Structural Monitoring Systems*, Naples, Italy, 17-18 September 2014.
[6] Woodhouse J 1998 Linear damping models for structural vibration *Journal of Sound and Vibration* 215(3) pp 547–569.
[7] Iezzi F and Valente C 2018 Mode shapes complexity for damage identification of structures experiencing plasticization *Proceedings of the 9th International Conference on Computational Methods* vol 5(2018) pp 19–28 (ScienTech Publisher), 9th ICCM, 6th-10th August, Rome, Italy.
[8] Lofrano E, Paolone A, Ruta G and Taglioni A 2017 Perturbation damage indicators based on complex modes *Procedia Engineering* 199(2017) pp 1949–1954.
[9] Iezzi F, Valente C and Zuccarino L 2015 The measure of the modal complexity as structural damage indicator (in Italian) *Proceeding of XVI ANIDIS Conference*, L'Aquila, Italy, 13-17 September 2015.
[10] Iezzi F, Spina D and Valente C 2015 Damage assessment through changes in mode shapes due to non-proportional damping *Journal of Physics: Conference Series* 628(2015) 012019.
[11] Friswell M I and Motthershead J E 1995 *Finite Element Model Updating in Structural Dynamics* (Netherlands: Kluwer Academic Publshers).
[12] Flanigan C C 1998 Model reduction using Guyan, IRS and dynamic methods. *Proceedings of the 16th International Modal Analysis Conference*, 2-5 February, Santa Barbara, CA, pp 172–176.
[13] Ewins D J 1986 *Modal Testing: Theory and Practice* (England: Research Studies Press Ltd).
[14] Adhikari S 2014 *Structural Dynamics Analysis with Generalized Damping Models: Analysis* (UK:ISTE/USA:Wiley).
[15] Meirovitch L 1980 *Computational Methods in Structural Dynamics* (Netherlands: Sijthoff & Noordhoff).
[16] Liu K, Kujath M R and Zheng W 2000 Quantification of non-proportionality of damping in discrete vibratory systems *Computers and Structures* 77 pp 557–569.
[17] Allemang R J and Brown D L 1982 A correlation correlation coefficient for modal vector analysis *Proceedings of the 1st International Modal Analysis Conference*, 8-10 November, Orlando, Florida, pp 110–116.